cross sections than the corresponding reactions by $H_2S^+ + H_2S$. Moreover, the substantial differences observed between the spectra of S_2^+, HS_2^+, and $H_2S_2^+$ shown in Figure 5 and those in Figure 6 support the conclusion that reactions 20–23 contribute little to the spectra observed in Figure 5. The above investigation also demonstrates the importance of using the differential pumping arrangement for the study of unimolecular decompositions of dimer and cluster ions such as reactions 1–6.

The adiabatic IEs for the $\tilde{A}^2A_1$ and $\tilde{B}^2B_2$ states of H_2S^+ obtained by photoelectron spectroscopy[30] are 12.777 eV (970 Å) and 14.643 eV (847 Å), respectively. The AEs for the S_2^+, $H_2S_2^+$, and $H_3S_2^+$ ions are found to be close to the IE of the $\tilde{A}^2A_1$ state. As the photon energy increases to approximately the IE of the $\tilde{B}^2B_2$ state, the PIE curves for the S_2^+, HS_2^+, $H_2S_2^+$, and $H_3S_2^+$ all exhibit further increases in PIE. Qualitatively, one may conclude that reactions 1–5 proceed with higher probabilities when the H_2S^+ moiety in $H_2S^+ \cdot H_2S$ is prepared in the $\tilde{A}^2A_1$ and $\tilde{B}^2B_2$ states than when H_2S^+ is formed in the $\tilde{X}^2B_1$ state. Furthermore, since the productions of S^+ and HS^+ are believed to arise from fast predissociation of H_2S^+, it is likely that many of the fragmentation reactions might be stepwise processes such as

$$H_2S^+ \cdot H_2S \rightarrow S^+ \cdot H_2S + H_2 \rightarrow S_2^+ + 2H_2 \quad (24)$$

$$\rightarrow S^+ \cdot H_2S + H_2 \rightarrow HS_2^+ + H_2 + H \quad (25)$$

$$\rightarrow HS^+ \cdot H_2S + H \rightarrow HS_2^+ + H_2 + H \quad (26)$$

$$\rightarrow HS^+ \cdot H_2S + H \rightarrow H_2S_2^+ + 2H \quad (27)$$

In order to measure the relative reaction probabilities of reactions 1–5 as a function of ionizing photon energy without the interference of processes such as reactions 14–18, it is necessary to operate the H_2S nozzle beam under conditions that minimize the formation of hydrogen sulfide trimers and higher clusters. The intensities for $(H_2S)_2^+$, $H_3S_2^+$, H_3S^+, $H_2S_2^+$, HS_2^+, and S_2^+ were measured at $P_0 \approx 200$ torr and $T_0 \approx 230$ K at wavelength intervals of 50 Å in the region 650–950 Å. Under these beam conditions, the intensities of $H_5S_2^+$, $(H_2S)_3^+$, and higher hydrogen sulfide cluster ions were all found to be within the noise level, indicating that the concentrations of $(H_2S)_n$, $n \geq 3$, were negligible. After careful corrections for isotopic contributions, the true intensities for $(H_2S)_2^+$, $H_3S_2^+$, H_3S^+, $H_2S_2^+$, HS_2^+, and S_2^+, were obtained. The differences in transmission of these ions through the mass spectrometer used in this experiment have not been corrected for. Since the masses of these ions with the exception of H_3S^+ differ only by a few mass units, the transmission factors are expected to have minor effects on the measured relative intensities of $(H_2S)_2^+$, $H_3S_2^+$, $H_2S_2^+$, HS_2^+, and S_2^+. The relative abundances, $I[(H_2S)_2^+]/\sum$, $I(H_3S_2^+)/\sum$, $I(H_3S^+)/\sum$, $I(H_2S_2^+)/\sum$, $I(HS_2^+)/\sum$, and $I(S_2^+)/\sum$ for $(H_2S)_2^+$, $H_3S_2^+$, H_3S^+, $H_2S_2^+$, HS_2^+, and S_2^+, respectively, in percentage as a function of photon energy in the region 650–950 Å are plotted in Figure 7. Here $I[(H_2S)_2^+]$, $I(H_3S_2^+)$, $I(H_3S^+)$, $I(H_2S_2^+)$, $I(HS_2^+)$, and $I(S_2^+)$ represent the true intensities of $(H_2S)_2^+$, $H_3S_2^+$, H_3S^+, $H_2S_2^+$, HS_2^+, and S_2^+, respectively, and $\sum$ is the sum of $I[(H_2S)_2^+]$, $I(H_3S_2^+)$, $I(H_3S^+)$, $I(H_2S_2^+)$, $I(HS_2^+)$, and $I(S_2^+)$. As shown in Figure 7, $H_3S^+ + HS$ is found to be the dominate product channel with only minor variation in fragmentation probability in this region. This analysis also confirms the above conclusions that the $S_2^+ + 2H_2$, $HS_2^+ + H_2 + H$, $H_2S_2^+ + H_2$, and $H_3S_2^+ + H$ are weak product channels that have higher reaction probabilities when H_2S^+ in $H_2S^+ \cdot H_2S$ is formed in the $\tilde{A}^2A_1$ or $\tilde{B}^2B_2$ states.

In summary, the study of the unimolecular decomposition of $(H_2S)_2^+$ using the molecular beam photoionization method has allowed the unambiguous identification of the S_2^+, HS_2^+, $H_2S_2^+$, H_3S^+, and $H_3S_2^+$ ions to be the primary product ions from the reactions of $H_2S^+ + H_2S$. From the AE and IE measurements of various ions, the energetics of HS_2^+, $H_3S_2^+$, $H_5S_2^+$, H_3S^+, $(H_2S)_2^+$, and $(H_2S)_3^+$ have been calculated. This study also reveals that the ion–molecule reactions between H_2S^+ and H_2S to form S_2^+, HS_2^+, $H_2S_2^+$, and $H_3S_2^+$ are strongly favored for H_2S^+ in the $\tilde{A}^2A_1$ and $\tilde{B}^2B_2$ states in comparison to the $\tilde{X}^2B_1$ state. Furthermore, the decompositions of the $H_2S^+ \cdot H_2S$ complexes to form S_2^+, HS_2^+, and $H_2S_2^+$ are likely to proceed by stepwise processes as shown in reactions 24–27.

Acknowledgment. We thank Dr. Y. Ono and Dr. S. H. Linn for their assistance in obtaining part of the data of this experiment.

Registry No. $H_5S_2^+$, 62873-60-3; $H_3S_2^+$, 68941-81-1; $H_2S_2^+$, 63228-83-1; HS_2^+, 63228-82-0; S_2^+, 12597-02-3; H_3S^+, 18155-21-0; H_2S, 7783-06-4; H_2S^+, 26453-60-1; H, 12385-13-6; H_2, 1333-74-0.

Analysis of Fully Anisotropic Overall Molecular Tumbling with Group Internal Rotation: Steroid Examples

George C. Levy,* Anil Kumar, and Dehua Wang

Contribution from the N.I.H. Resource for Multi-Nuclei NMR and Data Processing, Chemistry Department, Syracuse University, Syracuse, New York 13210. *Received April 5, 1983*

Abstract: The theory for fully anisotropic overall motion with internal rotation is presented and applied to substituted 5α-androstane steroids to compute the diffusion constants for overall motion as well as internal CH_3 rotations. It is found that calculations give close fits with the experimental data. Although existing literature discusses steroid motion in terms of isotropic or axially symmetric motion, it was found in all cases that the androstane skeletons reorient anisotropically. In two of six compounds studied, overall motion was close to axially symmetric; in the remaining molecules the three diffusion constants were significantly different. Calculations of rotational rates for the C-18 and C-19 methyl groups showed relatively fast spinning of C-19.

Carbon-13 spin–lattice relaxation times (T_1) have been widely used to investigate details of molecular motion in solution.[1-4] A rigid molecule that is not spherically symmetric will generally undergo anisotropic rotation.[1-7] The anisotropy of rotation can arise from inertial differences and because the asymmetric (often assumed ellipsoidal) shape of the molecule has variable requirements for reorientation within the solvent "cage" (e.g., solvent molecules must be translated for motions about axes perpendicular

(1) Wright, D. A.; Axelson, D. E.; Levy, G. C. In "Topics in Carbon-13 NMR Spectroscopy"; Levy, G. C., Ed.; Wiley-Interscience: New York, 1979; Vol. 3, Chapter 2, and references cited therein.
(2) Komoroski, R. A.; Levy, G. C. *J. Phys. Chem.* **1976**, *80*, 2414.
(3) Howarth, O. W. *J. Chem. Soc., Perkin Trans. 2* **1982**, 263.
(4) Levy, G. C.; Cargioli, J. D.; Anet, F. A. L. *J. Am. Chem. Soc.* **1973**, *95*, 1528.
(5) Beierbeck, H.; Martino, R.; Saunders, J. K. *Can. J. Chem.* **1980**, *58*, 102.
(6) (a) Axelson, D. E.; Holloway, C. E. *Can. J. Chem.* **1980**, *58*, 679. (b) Somorjai, R. L.; Deslauriers, R. *J. Am. Chem. Soc.* **1976**, *98*, 6460.
(7) Levy, G. C.; Craik, D. J.; Phan Viet, M. T.; Dekmezian, A. *J. Am. Chem. Soc.* **1982**, *104*, 25.

0002-7863/83/1505-7536$01.50/0

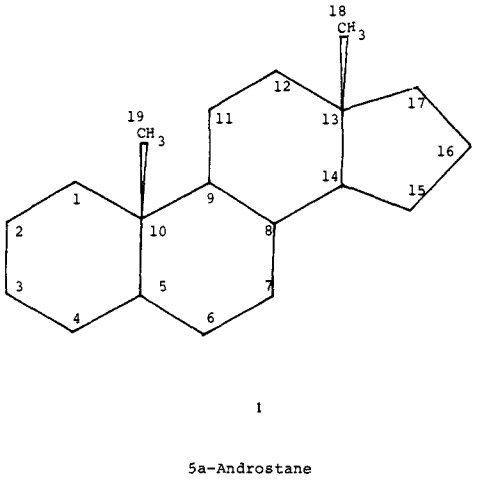

1

5a-Androstane

Figure 1. 5α-Androstane.

to the principal axes). ^{13}C T_1 data can be used to obtain rotational diffusion constants R_1, R_2, and R_3 about the principal axes. The diffusion constants are generally derived from application of Woessner's equations for ellipsoids.[8]

For moderate-sized organic molecules undergoing anisotropic motion with or without internal motion, it is necessary to measure T_1 and NOE for many *different* carbons to uniquely define the dynamics. In principle, the data for as few as 10 distinct carbon–hydrogen internuclear vectors that sample the orientational space of the molecule adequately permits the determination of principal axes as well as the diffusion constants of the molecular motion. In practice, many more C–H vectors may be required to define a solution.

We have written a computer program, MOLDYN,[9] which allows group rotational rates to be determined in the presence of totally anisotropic overall tumbling. Given the atomic coordinates and masses for a molecule, the program can compute the principal axes and moments of the inertia and rotate the axes through the appropriate Euler angles so that the inertial tensor is diagonalized. Then on the assumption that both inertial and diffusion tensors are diagonal simultaneously, the diffusion constants can be computed.

In studies of anisotropic motion is nonsymmetrical molecules it is unsually assumed that the inertial axis system can be used to characterize motion, but recent work[6] has shown the importance of interacting substitutent groups in shifting the diffusion axis system away from the inertial axis system. However, in such a case, the calculation of the relative orientation of the two-coordinate systems as well as the new oriented diffusion tensor is not trivial and is liable to nonunique solutions and possible misinterpretation. With careful interpretation, knowledge of the diffusion axes and the diffusion tensor can provide important new understanding of the way molecules interact in solution. In a previous paper,[7] we reported that the rigid 6-X-benzonorbornyl system acts as a motional dynamics probe for anisotropic motion. The benzonorbornyl probe molecule is not, however, ideal for the present purpose since there are only 11 C–H vectors—8 protonated carbon T_1s available to optimize six variables. Instead, the rigid androstane steroid skeleton (Figure 1) was chosen, specifically because it has 26 usable C–H vectors (15 skeletal CH or CH_2 carbons) arranged along a long and largely rigid frame.

In 1971, Allerhand published a landmark paper describing ^{13}C spin–lattice relaxation of several compounds, including the steroid cholesteryl chloride.[10] In that paper the motion of the steroid was interpreted as isotropic. But in a later paper, ApSimon et al.[11] found that the NT_1 of C-3 of many androstane examples is less than that observed for other ring carbons. The long steroidal axis passes through or very close to C-3; thus the rotation rate about this axis is expected to be more rapid than about any other axis. In their calculations, an effective correlation time

$$\frac{1}{T_1} = \frac{N\hbar^2 r_C^2 r_H^2}{r_{C\text{-}H}^6}\tau_c \qquad (1)$$

was used as a first approximation to calculate methyl internal rotation rates.

In this paper we present a theory for fully anisotropic overall motion with internal rotation and then apply it to the substituted steroids to determine diffusion constants for overall motion and internal rotation of methyl groups. The available theoretical treatments of anisotropic tumbling require extension to allow calculation of methyl group rotation. Although internal motion modeled as a rotation or three-site jump superimposed onto axially symmetric overall motion had been considered by Woessner,[12] it is only recently that the case for fully anisotropic overall with internal motion had been considered. Tsutsumi,[13] Ban,[14] and Bluhm[15] have modeled internal motion as two- and three-site jump motions superimposed onto fully anisotropic overall motion. Levine et al.[16] have addressed the problem of multiple internal rotations superimposed onto fully anisotropic overall motion. However they assumed all bond angles as identical and therefore their expression cannot be reduced to the case of methyl group rotations. London and Avitabile[17] and Deslauriers and Somorjai[18] then extended Levine et al's results to multiple internal rotation with nonidentical bond angles. In both papers, although the correct expressions were obtained, no indication was given that the results were also valid for the fully anisotropic overall motion. In fact, both groups of authors consider their expressions valid for axially symmetric overall motion and give only the eigenvalues for that case.[17,18]

Theory

Fully Anisotropic Motion. If magnetic dipole–dipole interactions between ^{13}C nuclei and protons dominate spin–lattice relaxation for ^{13}C nuclei in the compound, then relaxation rates depend mainly on the number of attached protons and the modulation of the interactions by molecular motion of the C–H bond vectors. The magnetic dipole–dipole nuclear spin–lattice relaxation time (T_1) of two nuclei having constant internuclear separation r_{CH} can be expressed as

$$\frac{1}{T_1^{DD}} = \left(\frac{1}{10}\right)\frac{\gamma_H^2\gamma_C^2\hbar^2}{r_{C\text{-}H}^6}[J(\omega_H - \omega_C) + 3J(\omega_C) + 6J(\omega_H + \omega_C)] \qquad (2)$$

where the γ terms are the magnetogyric ratios, $\hbar$ is Planck's constant divided by 2π, and ω_i is the angular resonance frequency. $J(\omega_i)$ is the spectral density function obtained by Woessner,[8] assuming a rigid molecule tumbling anisotropically in solution:

$$J(\omega_i) = \frac{12Rd(\omega_i^2 + 36L^2)}{(1/\tau_+^2 + \omega_i^2)(1/\tau_-^2 + \omega_i^2)} - \frac{12e(\omega_i^2 - 36L^2)}{(1/\tau_+^2 + \omega_i^2)(1/\tau_-^2 + \omega_i^2)} + \frac{C_1\tau_1}{(1 + \omega_i^2\tau_1^2)} + \frac{C_2\tau_2}{(1 + \omega_i^2\tau_2^2)} + \frac{C_3\tau_3}{(1 + \omega_i^2\tau_3^2)} \qquad (3)$$

(8) Woessner, D. E. *J. Chem. Phys.* **1962**, *37*, 647.
(9) Craik, D. J.; Kumar, A.; Levy, G. C. *J. Chem. Inf. Comput. Sci.* **1983**, *23*, 30.
(10) Allerhand, A.; Doddrell, D. Komoroski, R. A. *J. Chem. Phys.* **1971**, *55*, 189.
(11) ApSimon, J. W.; Beierbeck, H.; Saunders, J. K. *Can. J. Chem.* **1975**, *53*, 338.
(12) Woessner, D. E.; Snowden, B. S., Jr.; Meyer, G. H. *J. Chem. Phys.* **1969**, *50*, 719.
(13) Tsutsumi A. *Mol. Phys.* **1979**, *37*, 111.
(14) Ban, B. *J. Magn. Reson.* **1981**, *45*, 118.
(15) Bluhm, Th. *Mol. Phys.* **1982**, *47*, 475.
(16) Levine, Y. K.; Birdsall, N. J. M.; Lee, A. G.; Metcalfe, J. C.; Partington, P.; Roberts, G. C. K. *J. Chem. Phys.* **1974**, *60*, 2890.
(17) London, R. E.; Avitabile, J. *J. Chem. Phys.* **1976**, *65*, 2443.
(18) Deslauriers, R.; Somorjai, R. L. *J. Am. Chem. Soc.* **1976**, *98*, 1931.
(19) Levy, G. C.; Lichiter, R. L.; Nelson, G. L. "Carbon-13 Nuclear Magnetic Resonance"; Wiley-Interscience: New York, 1980; Chapter 8.

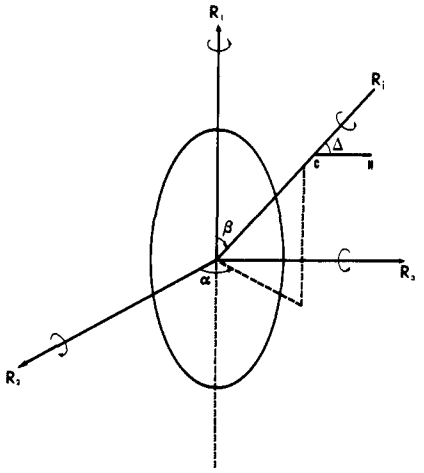

Figure 2. Nomenclature for the fully anisotropic overall motion with internal rotation model.

where the symbols are the same as in ref 7. Using a nonlinear SIMPLEX optimization algorithm, the computer program MOLDYN can determine those diffusion constants that minimize the sum of the squares of the deviations of the calculated and observed dipolar T_1 values.

Axially Symmetric Overall Motion with Internal Rotation. If the calculated anisotropic diffusion constants, R_1, R_2, and R_3 show that two of them are essentially equal, it is reasonable to assume that the molecular motion is dominated by axially symmetric tumbling. Methyl internal rotation constants may be determined by application of Woessner's equations for axially symmetric ellipsoids:

$$J(\omega_i) = K_h[B_{A1}f_h(\tau_A) + B_{A2}f_h(\tau_{A2}') + B_{A3}f_h(\tau_{A3}') + B_{B1}f_h(\tau_B) + B_{B2}f_h(\tau_{B2}') + B_{B3}f_h(\tau_{B3}') + B_{C1}f_h(\tau_C) + B_{C2}f_h(\tau_{C2}') + B_{C3}f_h(\tau_{C3}')] \quad (4)$$

where the various terms are defined in ref 12. Equation 4 is a special case of eq 9 presented in the next section on fully anisotropic overall motion with internal motion.

Fully Anisotropic Overall Motion with Internal Rotation. The correlation function for fully anisotropic overall motion with internal rotation can be written as the product of correlation functions for the overall motion and that for internal motion, provided that the two motions can be considered independent and uncorrelated.[20] The total correlation function is then

$$C(t) = \sum_q\sum_a\sum_{a'}\sum_b\sum_{b'}\langle D^{(2)}_{qa}{}^*(\Omega_{LD}, 0)\, D^{(2)}_{qa'}(\Omega_{LD},t)\rangle \exp[i(a - a')\alpha] d^{(2)}_{ab}(\beta) d^{(2)}_{a'b}(\beta) \langle \exp[i(b - b')\gamma]\rangle d^{(2)}_{b0}(\Delta) d^{(2)}_{b'0}(\Delta) \quad (5)$$

The indicies run from −2 to 2 and $D^{(2)}$ and $d^{(2)}$ are second-order Wigner and reduced Wigner rotation matrices.[21] The angular brackets denote ensemble averages, the first representing the overall motion and the second the internal rotation about a single axis making Euler angles α and β with a system of axes fixed in the molecule (Figure 2). The C–H internuclear vector makes an angle Δ with the internal axis of rotation. The time-dependent random variables are the Euler angles $\Omega_{LD} = (\alpha_{LD}, \beta_{LD}, \gamma_{LD})$ which the molecular principal axes make with laboratory axes, and γ is the angle of rotation about the internal axis of rotation. For overall motion the rotational correlation function for a body with arbitrary shape has been obtained by Hubbard[22] as

$$C_O(t) = \langle D^{(2)}_{qa}{}^*(\Omega_{LD},0) D^{(2)}_{q'a}(\Omega_{LD},t)\rangle = \delta_{qq'}(1/5)\sum_{r=-2}^{2}\exp(-\lambda_r t) Z(\lambda_r)_{aa'} \quad (6)$$

Hubbard gives explicit expressions for the eigenvalues λ_r and the matrix Z of eigenvectors. The Hubbard formulation is mathe-

(20) Wallach, D. *J. Chem. Phys.* **1967**, *47*, 5258.
(21) Rose, M. E. "Elementary Theory of Angular Momentum"; Wiley: New York, 1957; Chapter 4.
(22) Hubbard, P. S. *J. Chem. Phys.* **1970**, *52*, 563.

Table I. 90.56-MHz ^{13}C NMR T_1 Data for 5α-Androstane Derivatives and Methyl Methoxypodocarpate[a]

		T_1[b]													NT_1[c]	
compd		C-1	C-2	C-3	C-4	C-5	C-6	C-7	C-8	C-9	C-11	C-12	C-13	C-14	C-15	C-16	C-17	C-18	C-19
5α-androstane (1)	obsd	2.2	2.0	1.7	2.3	3.8	2.3	2.2	3.8	3.8	2.0	2.1		3.9	2.1	2.1	2.4	10.2	16.2
	calcd	2.2	2.1	1.5	2.2	3.9	2.2	2.1	3.9	3.9	2.1	2.2		4.0	2.2	2.0	2.1	10.2	16.2
5α-androstan-17-one (2)	obsd	1.5	1.4	1.1	1.4	2.7	1.4	1.4	2.5	3.2	1.4	1.4		3.4	1.4	1.5		8.7	17.4
	calcd	1.5	1.4	1.2	1.4	2.8	1.5	1.4	2.8	2.8	1.4	1.5		2.9	1.3	1.3		8.7	17.4
5α-androstan-3β-ol (3)	obsd	1.1	1.2	1.8	1.1	1.9	1.1	1.1	1.9	1.9	1.2	1.1		1.8	1.2	1.3	1.0	8.4	13.5
	calcd	1.1	1.1	1.8	1.2	1.9	1.1	1.1	1.9	1.9	1.1	1.1		1.9	1.1	1.1	1.2	8.4	13.5
5α-androstane-3β,17β-diol (4)	obsd	0.81	0.82	1.7	0.90	1.7	0.80	0.78	1.4	1.5	0.80	0.84		1.6	0.77	0.91	1.4	7.5	10.5
	calcd	0.81	0.80	1.5	0.80	1.5	0.81	0.80	1.5	1.6	0.80	0.82		1.6	0.80	0.83	1.6	7.5	10.5
5α-androstane-3α,17β-diol (5)	obsd	0.64	0.60	1.0	0.71	1.2	0.65	0.62	1.2	1.1	0.58	0.64		1.2	0.63	0.63	1.1	8.4[d]	
	calcd	0.64	0.61	1.1	0.65	1.1	0.64	0.61	1.1	1.1	0.61	0.65		1.2	0.63	0.59	1.2	8.4	
methyl methoxypodocarpate (6)	obsd	0.65	0.63	0.53		1.1	0.68				1.1		0.87	1.3	0.70		1.0	8.4	7.5
	calcd	0.61	0.64	0.54		1.2	0.63				1.2		0.87	1.2					

[a] T_1 values in s. [b] T_1 values are calculated according to eq 8. [c] T_1 values are calculated according to this paper, with $\alpha = \beta = 90°$ and $\Delta = 70.5°$ (see Figure 2). [d] Two peaks are overlapped.

Table II. Calculated Diffusion Constants ($\times 10^{-10}$ s^{-1})

compd	diffusion const[a] R_1	R_2	R_3	ratio of $R_1:R_2:R_3$	R_i[b] C-18	C-19	solvent	concn, mol
5α-androstane	3.9	1.0	0.52	7.5:1.9:1	6.9	19.2	$DCCl_3$	0.50
5α-androstan-17-one	1.6	0.74	0.77	2.1:0.96:1	7.7	38.4	$DCCl_3$	0.50
5α-androstan-3β-ol	2.9	0.41	0.15	19:2.7:1	10.3	43.2	$DCCl_3$	0.50
5α-androstane-3β,17β-diol	1.6	0.20	0.26	6.2:0.77:1	11.1	31.9	D_3COD	0.044
5α-androstane-3α,17β-diol	1.2	0.26	0.13	9.2:2.0:1	29.2		D_3COD	0.044
methyl methoxypodocarpate	0.70	0.29	0.34	2.1:0.85:1			$DCCl_3$	0.80

[a] Calculated according to eq 8. [b] R_i is internal rotation of methyl groups with $\alpha = \beta = 90°$ and $\Delta = 70.5°$ (cf. Figure 2).

matically equivalent to that obtained by Woessner,[8] although the former is more convenient for combining overall and internal motions because of its matrical form.

For the diffusion of an axially symmetric cylinder the above reduces to

$$C_O(t) = \delta_{qq'}\delta_{aa'}(1/5)\exp(-\lambda_a t) \quad (7)$$

where $\lambda_a = 6R_2 + a^2(R_1 - R_2)$.

The correlation function for internal rotation is given by

$$C_I(t) = \langle \exp[i(b - b')\gamma] \rangle = \delta_{bb'}\exp(-b^2 R_i t) \quad (8)$$

Which is easily obtained by substituting $R_2 = 0$ in the expression for an axially symmetric cylinder. The Fourier transform of the total correlation function is then the spectral density:

$$J(\omega_i) = \sum_a \sum_{a'} \sum_b \sum_r Z(\lambda_r)_{aa'} D^{(2)}_{ab}{}^*(\alpha,\beta,0) D^{(2)}_{a'b}(\alpha,\beta,0) \times [d^{(2)}_{b_0}(\Delta)]^2 \frac{\lambda_r + b^2 R_i}{(\lambda_r + b^2 R_i)^2 + \omega_i^2} \quad (9)$$

where the indices run from −2 to 2. For axially symmetric overall motion the above reduces to eq 4. Extension to multiple internal rotations is straightforward.

Experimental Section

All compounds used were obtained commercially. Solutions for NMR were prepared in $DCCl_3$ or D_3COD, nitrogen bubbled for 15–20 mins, and sealed in 10-mm tubes. ^{13}C spectra (90.56 MHz) with broad-band proton decoupling were obtained on a Bruker WM-360 wide-bore FT NMR spectrometer. T_1 data were obtained by using the FIRFT[19] technique, with delay times of 3 s between the −(180–τ–90–)− sequences. A total of 15 τ values ranging from 0.01 s to $5T_1$ s were used to obtain each data set. The T_1 values given in Table I are each determined from two experiments and are accurate to ±5%. NOE measurements showed full enhancement for all protonated ring carbons, confirming the dominance of dipolar relaxation at these sites.

Calculations

Al computations were done by using our recently developed programm MOLDYN.[9] This program enables a scientist to explore over 22 molecular motional models. Best fits to experimental data were obtained by the Simplex nonlinear least-squares optimization algorithm implemented in the MOLDYN system.

The molecular coordinates were obtained by using standard bond lengths and bond and torsion angles, assuming chair conformations for the rigid steroid skeleton rings. A Dreiding model was used as a visual aid for confirming orientations of torsion angles. We believe that the coordinates obtained were sufficiently accurate for these computations.

The diffusion constants were calculated, assuming that the inertia and diffusion tensors were simultaneously diagonal. For the overall motion this reduces the number of unknowns to three from six. The number and quality of data do not allow reliable computation of the reorientational Euler angles—if other than zero—between the two tensors.

Results and Discussion

Diffusion constants for androstane systems were determined from T_1's of the protonated skeletal carbons using MOLDYN[9] (Table I). For calculations involving the simultaneous fitting of T_1 values, the maximum variation between calculated and observed values was less than 15%; most deviations were less than 5% (Table I).

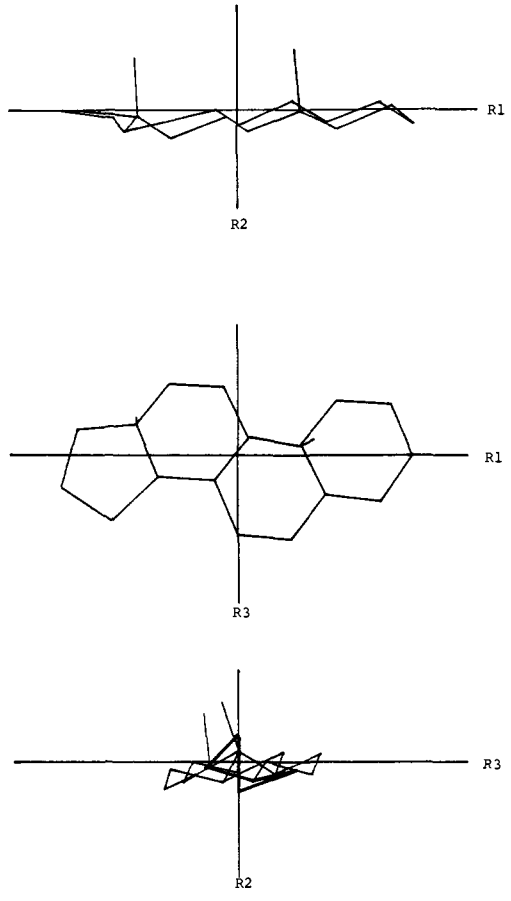

Figure 3. Orientation of principal axes of inertia in 5α-andorstane: R_2 perpendicular to molecular plane, R_1 along the longest molecular axis.

For 10% error in representative T_1 values, the calculated diffusion constants varied by 10 to 20%, depending on the carbon location.

Table II summarizes the calculated diffusion constants, assuming the inertial frame identity. The orientation of the principal axis system for 5α-androstane is shown in Figure 3. The principal axes for the other steroids do not differ significantly from that of 5α-androstane. Therefore, the parameters $\alpha = \beta = 90°$ and $\Delta = 70.5°$ were used for all compounds in the calculation of methyl rotation rates.

Early reports[10,11] indicated that steroids appeared to undergo isotropic overall dynamics, with rapid CH_3 rotations allowed. In a 1975 study[23] we determined that methyl methoxypodocarpate (**6**) and, to a lesser extent, cholesteryl chloride showed evidence of anisotropic overall motion. The calculated anisotropic diffusion of 6 shown in Table II indicates that the rotation rate about the R_1 axis is, approximately 2 times faster than about the R_3 axis.

Analysis of the data listed in Table II reveals several important features. Unsubstituted 5α-androstane undergoes typical anisotropic rotation, the principal molecular, axis, R_1, having the fastest diffusion constant, followed by R_2 (perpendicular to the "molecular plane"), with R_3 being the smallest. The ratio of $R_1:R_2:R_3$ in this

(23) Levy, G. C.; Edlund Ulf *J. Am. Chem. Soc.* **1975**, *97*, 5031.

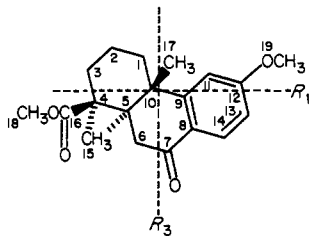

6

hydrocarbon is 7.5:1.9:1, which correlates with its ellipticities.

5α-Androstan-17-one, (**2**) still essentially follows elliptic diffusional behavior with fastest rotational diffusion constant around R_1. However, the carbonyl group introduces polar properties, which cause **2** to be strongly solvated in $DCCl_3$ solution. Slower rotational diffusion around R_1 and a lower ratio for the three diffusion constants to 2.1:≈1.0:1 show that solvation and electrostatic considerations affect molecular dynamics.

5α-Androstan-3β-ol (**3**) is expected to associate via intermolecular hydrogen bonding. The rotational ratio about its three principal axes, R_1:R_2:R_3, is 19:2.7:1. This result indicates that solution dimerization or "polymerization" of 5α-androstan-3β-ol strongly restricts rotation about the R_3 axis.

5α-Androstane-3β,17β-diol (**4**) and 5α-androstane-3α-17β-diol (**5**) have hydroxyl groups at each end of the long molecular axis of the compound. **4** and **5** were dissolved in D_3COD as solubility was very limited in $CDCl_3$. As shown in Table II, rotation rates about both R_2 and R_3 axes are significantly decreased. Unlike the situation for compounmd **3** in $CDCl_3$ the presence of 3β-and 17β-hydroxyl groups in **4** does not result in increased motional anisotropy. In the case of **4** the concentration is much lower, and the solvent will partially suppress intermolecular association of the steroid molecules.

Table II shows that the diffusion constants R_2 and R_3 for 5α-androstan-17-one and 5α-androstane-3β,17β-diol are very close, implying that axially symetric motion is a reasonable approximation for both of these compounds. The other androstane derivatives, however, rotate fully anisotropically.

Methyl Group Rotation. Calculated internal rotation rates of methyl groups using the method developed in this paper are listed in Table II. When fully anisotropic overall motion is utilized, the internal rotation rates of methyl groups C-18 and C-19 of the 5α-androstane deriviatves range from 6.9×10^{10} s^{-1} to 4.3×10^{11} s^{-1}. However, using isotropic overall motion with the internal rotation model ApSimon et al.[11] found methyl group rotation rates which are 2–3 times smaller (2.3×10^{10} s^{-1} to 2.8×10^{11} s^{-1}).

Generally, as indicated in Table II, we have determined that C-19 rotates faster than does C-18. This fact can be explained by the interaction between the steroid axial hydrogens and the two methyl groups. Methyl group C-19 has five axial hydrogens which surround it fairly symmetrically, whereas C-18 has only two axial hydrogens located on one side. The asymmetric placement of axial hydrogens may provide a rotameric energy well, slowing down internal rotation of C-18. The internal rotation rates of C-18 and C-19 vary somewhat with substituents. Using these calculated diffusion constants for internal rotation, one can calculate the energy barriers for $-CH_3$ group rotation by the Arrhenius equation.[24] The average values of rotation barriers for C-18 and C-19 are 3.0 and 2.3 kcal/mol, respectively.

Proton NMR has also been employed to determine methyl group internal rotational diffusion. For example, Hall and Sanders report[25] that in 11β-hydroxyprogesterone proton data on CH_3-19 and CH_3-18 are consistent with our conclusion that the former rotates faster than the latter except in 1,2-didehydrostestosterone where ring A unsaturation reduces the axial interactions with CH_3-18, so speeding its rotation. However, of necessity the ^1H study assumed isotropic tumbling for the rigid steroid framework, which is contrary to the results of our detailed quantitative analysis.

Acknowledgment. This work was supported by the National Science Foundation (Grant CHE 8105109). The development of the program MOLDYN was supported through Grant RR-01317, awarded by the Division of Research Resources, National Institutes of Health. Prof. Werner Herz kindly supplied a sample of methyl methoxypodocarpate. Dehua Wang thanks Dr. D. J. Craik for the help with the computation of molecular geometry data. We also thank Dr. Th. Bluhm for sending a preprint of his paper and Anirban Banerjee for technical assistance.

Registry No. 1, 438-22-2; **2**, 963-74-6; **3**, 1224-92-6; **4**, 571-20-0; **5**, 1852-53-5; **6**, 901-36-0.

(24) Berger, S.; Kreissl, F. R.; Grant, D. H.; Robberts, J. D. *J. Am. Chem. Soc.* **1975**, *97*, 1805.

(25) (a) Hall, L. D.; Sanders, J. K. M. *J. Org. Chem.* **1981**, *46*, 1132. (b) Hall, L. D., Sanders, J. K. M. *J. Am. Chem. Soc.* **1980**, *102*, 5703.